

Universal First-Passage-Time Distribution of Non-Gaussian Currents

Shilpi Singh,^{1,*} Paul Menczel,¹ Dmitry S. Golubev,¹ Ivan M. Khaymovich,^{2,3} Joonas T. Peltonen,¹
Christian Flindt,¹ Keiji Saito,⁴ Édgar Roldán,⁵ and Jukka P. Pekola¹

¹*QTF Centre of Excellence, Department of Applied Physics, Aalto University, 00076 Aalto, Finland*

²*Max Planck Institute for the Physics of Complex Systems, Nöthnitzer Strasse 38, 01187 Dresden, Germany*

³*Institute for Physics of Microstructures, Russian Academy of Sciences, 603950 Nizhny Novgorod, GSP-105, Russia*

⁴*Department of Physics, Keio University—Yokohama 2238522, Japan*

⁵*The Abdus Salam International Centre for Theoretical Physics, Strada Costiera 11, 34151, Trieste, Italy*

 (Received 18 September 2018; published 13 June 2019)

We investigate the fluctuations of the time elapsed until the electric charge transferred through a conductor reaches a given threshold value. For this purpose, we measure the distribution of the first-passage times for the net number of electrons transferred between two metallic islands in the Coulomb blockade regime. Our experimental results are in excellent agreement with numerical calculations based on a recent theory describing the exact first-passage-time distributions for any nonequilibrium stationary Markov process. We also derive a simple analytical approximation for the first-passage-time distribution, which takes into account the non-Gaussian statistics of the electron transport, and show that it describes the experimental distributions with high accuracy. This universal approximation describes a wide class of stochastic processes, and can be used beyond the context of mesoscopic charge transport. In addition, we verify experimentally a fluctuation relation between the first-passage-time distributions for positive and negative thresholds.

DOI: 10.1103/PhysRevLett.122.230602

Introduction.—The first-passage time is the time it takes a stochastic process to first reach a certain threshold. First-passage-time distributions have been studied in the context of Brownian motion [1–6], biochemistry [7–12], astrophysics [13,14], decision theory [15–17], searching problems [18,19], finance [20,21], and thermodynamics [17,22–27]. For example, in finance, the statistics of first-passage times is used in credit risk modeling, and in astrophysics, the distribution of times required for a star in a globular cluster to reach the escape velocity can be used to estimate the cluster’s lifetime [13]. In the context of mesoscopic electron transport, the interest in the distributions of first-passage times and waiting times [28,29] has been inspired by the tremendous progress in nanotechnology allowing very precise single-electron counting experiments [30–33]. Despite progress in the theory, no experimental study of the statistics of the time elapsed until the electric charge transferred through a conductor reaches a certain threshold has been reported so far.

The fluctuations of a stochastic process $N(t)$ are usually described in terms of the distribution $P_t(N)$ for the process to take the value N at a fixed time t . An alternative approach is to study the first-passage-time probability distribution $\mathcal{P}_N(t)$ for a stochastic process to first reach a given value N at time t . Recently, theories of the first-passage-time probability in Markovian systems have been developed [22,23]. They provide the first-passage-time probabilities for the net number of jumps between any two states of the

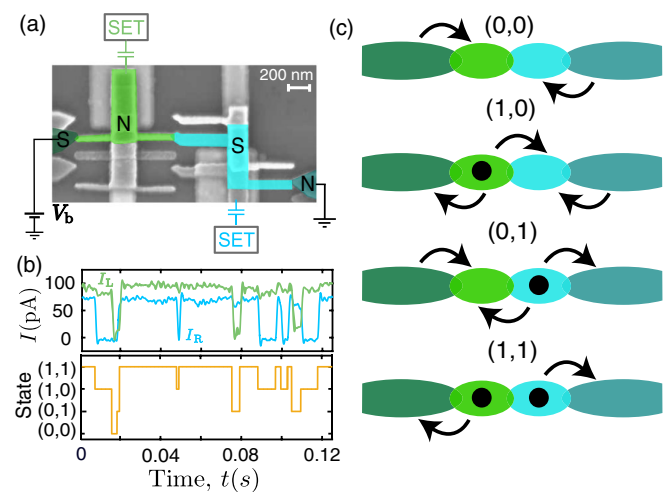


FIG. 1. Experimental setup. (a) Scanning electron micrograph of the double dot structure. A dc bias voltage $V_b = 90 \mu\text{V}$ is applied to the sample. One of the islands is made of normal metal (N , green), and the other one is superconducting (S , cyan). (b) Top panel: output currents of the detector SETs coupled to the left (I_L) and right (I_R) islands. Bottom panel: time resolved trajectory of the charge states of the system (N_L, N_R) , with $N_{L,R} = 0$ or 1 indicating, respectively, the absence or the presence of an extra electron in the corresponding island. (c) A schematic sketch of the double dot. The arrows show all possible transitions of electrons (black circles) in each charge state. The system is an example of an asymmetric simple exclusion process (ASEP) with two sites and open boundaries.

system. It has also been shown that first-passage-time distributions of currents [25,26,34] and stopping-time distributions of entropy production [17,24] satisfy universal laws for nonequilibrium steady-states obeying generalized detailed balance conditions. For such systems, the distributions for the first time to produce and reduce entropy by a given amount have the same shape [17,24]. This first-passage-time fluctuation relation was generalized to stochastic processes describing accumulation of evidence during sequential decision making [35,36]. As a result, the first-passage-time distribution for one-dimensional biased random walk obeys, similarly to a Brownian particle [1,2], the relation $\mathcal{P}_N(t) = \mathcal{P}_{-N}(t)e^{vN/D}$, with v and D being the drift and diffusion coefficients in a lattice of unit spacing [17].

In this Letter, we report an experimental study of the first-passage-time statistics for electrons transferred through a metallic double dot in the Coulomb-blockade regime. For this purpose, we obtain the full time record of millions of electron tunneling events between its two metallic islands (see Ref. [37] for details). Subsequently, we compute the first-passage-time distributions for the net number of electrons to reach a certain threshold. We find an excellent agreement with numerical calculations based on an exact theory [22,23]. We derive and experimentally verify a simple and universal analytical expression for the distribution $\mathcal{P}_N(t)$. It depends on only three parameters—the first three cumulants of the transferred charge distribution $P_t(N)$ and can be used to describe the first-passage-time fluctuations of a wide class of non-Gaussian stochastic processes. Finally, we test the first-passage-time fluctuation relation closely related to the fluctuation theorem for electron transport [38–43].

Experiment.—Our metallic double dot contains aluminum superconducting parts together with normal parts made of copper, see Fig. 1(a). The left lead and the right island are superconducting, while the left island and the right lead are normal. Thus, all three tunnel junctions connect a superconductor with a normal metal. The double dot has high normal state resistance of 55 M Ω . We run the experiment at the base temperature of 50 mK in the strong Coulomb blockade regime, where tunneling rates of electrons are very low, below 1 kHz. We monitor the direction of electron jumps using single-electron transistors (SETs) capacitively coupled to the islands.

The top panel of Fig. 1(b) shows time traces of electric currents of the two SETs. At chosen values of the gate potentials and at bias voltage $V_b = 90 \mu\text{V}$ applied to the device there exists four populated charge states (N_L, N_R), where $N_{L,R} = 0$ or 1 indicate the number of extra electrons in the islands. Monitoring the currents of both SETs, we detect the transitions between these states and find the corresponding transition rates. An example of a trajectory showing such transitions is shown in the bottom panel of Fig. 1(b). Figure 1(c) shows all possible transitions from

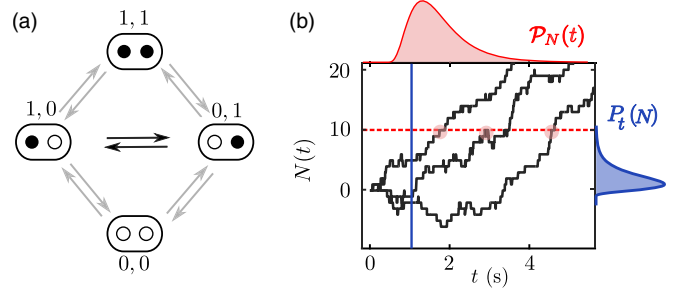


FIG. 2. Transition rates and first-passage times. (a) Depiction of the Markovian dynamics of the double dot system. The transition rates Γ_n^m from the state n to the state m have the following values: $\Gamma_{00}^{01} = 644$, $\Gamma_{01}^{00} = 131$, $\Gamma_{00}^{10} = 52$, $\Gamma_{10}^{00} = 39$, $\Gamma_{01}^{11} = 41$, $\Gamma_{11}^{01} = 43$, $\Gamma_{10}^{11} = 167$, $\Gamma_{11}^{10} = 53$, $\Gamma_{01}^{10} = 25$, and $\Gamma_{10}^{01} = 30$ Hz. We monitor the transitions between the states (1,0) and (0,1) shown by black arrows. (b) Black lines are time traces of the net number of electrons transferred through the middle junction from the right to the left island $N(t)$, horizontal dotted line indicates the threshold $N = 10$. First passage times are marked by red circles, and their distribution $\mathcal{P}_N(t)$ is illustrated by the red shaded area. Vertical blue line indicates the time t for which the distribution of the number of transferred electrons $P_t(N)$ is shown (blue shaded area, illustration).

every charge state [44]. The Markovian stochastic dynamics of the double dot is an example of an asymmetric simple exclusion process (ASEP) with two sites and open boundaries [45–49].

Since we have full information about the population of the islands at any time, we can monitor the transitions between all charge states. Here we are interested in electron tunneling events through the middle junction indicated by black arrows in Fig. 2(a). In Fig. 2(b), we plot three exemplary time traces of the net number of transmitted electrons $N(t)$. Next, we look at the first-passage times t_i at which the traces $N(t)$ cross a chosen threshold N , where i indicates different realizations of the experiment. The empirical distributions of these times for several values of the threshold $\mathcal{P}_N(t)$ are shown in Fig. 3. They constitute our main experimental result.

Theory.—First, we numerically calculate [50] first-passage-time distributions using an exact theory [22,23]. Experimentally determined transition rates between the charge states of the double dot, given in the caption of Fig. 2, are used as input parameters for the calculations. The results, shown by solid lines in Fig. 3, are in perfect agreement with the experiment, which confirms the consistency of our analysis.

Next, we propose a simple analytical expression for the first-passage-time distribution, which accounts for the non-Gaussian statistics of the electron transport via the third cumulant of the distribution $P_t(N)$. The cumulants of $P_t(N)$ are defined as $\mathcal{C}_n = (-i)^n \partial^n \mathcal{F}(\chi) / \partial \chi^n |_{\chi=0}$ [55], where $\mathcal{F}(\chi) = \lim_{t \rightarrow \infty} t^{-1} \ln [\sum_N e^{iN\chi} P_t(N)]$ is the cumulant generating function (CGF). In fact, if the observation time t

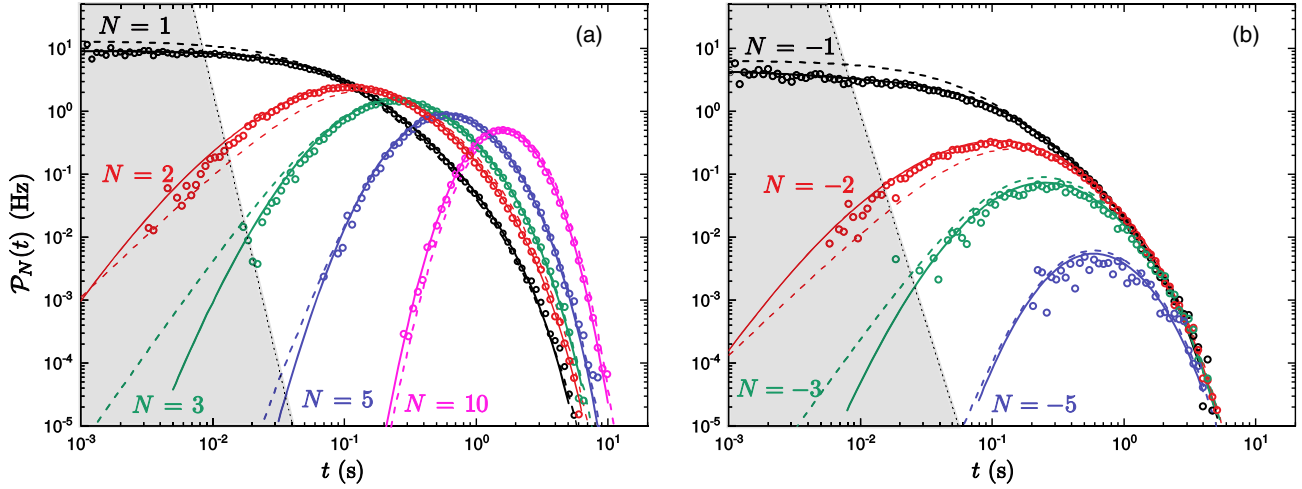


FIG. 3. First-passage-time distribution for positive (a) and negative (b) values of the threshold N . Different colors correspond to different values of the threshold indicated in the figure. Symbols are experimental data, solid lines—numerics based on the exact theory [22], dashed lines—Eq. (4). Shaded area approximately indicates the violation of the condition (5).

exceeds the time τ_r required for the system to relax to the steady state after a perturbation, the CGF becomes time independent. Thus, at $t \gtrsim \tau_r$ one finds

$$P_t(N) = \int_{-\pi}^{\pi} \frac{d\chi}{2\pi} e^{-iN\chi} e^{t\mathcal{F}(\chi)}. \quad (1)$$

One can expand the CGF in $i\chi$,

$$\mathcal{F}(\chi) = iC_1\chi - C_2\chi^2/2 - iC_3\chi^3/6 + \dots, \quad (2)$$

where $\mathcal{F}(0) = 0$ since the distribution $P_t(N)$ is normalized. At $t \gg C_3|N|/3C_2^2$, $P_t(N)$ becomes Gaussian since the last term $\sim \chi^3$ can be ignored. At shorter times this term results in a non-Gaussian $P_t(N)$, which does not have a simple analytical form. Therefore, we use another form of CGF allowing an analytical treatment. It models an asymmetric random walk with the step size α [3,51] or hopping of charged particles through a junction [52],

$$\mathcal{F}^{\text{arw}}(\chi) = \Gamma_+(e^{i\alpha\chi} - 1) + \Gamma_-(e^{-i\alpha\chi} - 1). \quad (3)$$

We adjust the rates Γ_{\pm} and the effective particle charge α in such a way that Taylor expansions of the functions (2) and (3) coincide up to the third order terms $\sim \chi^3$. Next, we solve the integral (1) using Eq. (3), and find the first-passage-time distribution $\mathcal{P}_N(t)$ from the equation [53] $P_t(N) = \int_0^t dt' \mathcal{P}_N(t') P_{t-t'}(0)$ (see Ref. [50] for details). Thus, we arrive at a simple analytical approximation,

$$\begin{aligned} \mathcal{P}_N(t) \simeq & \frac{|N^*| e^{-\frac{C_1 C_2 t}{C_3}} \left(\frac{C_2 + \sqrt{C_1 C_3}}{C_2 - \sqrt{C_1 C_3}} \right)^{\frac{N^*}{2}}}{t} \\ & \times I_{|N^*|} \left(\frac{C_1 \sqrt{C_2^2 - C_1 C_3}}{C_3} t \right), \end{aligned} \quad (4)$$

having the same structure as the random walk result (7). In this expression, $I_n(x)$ is the modified Bessel function of the first kind, and $N^* = [N\sqrt{C_1/C_3}]$ is the threshold value for the number of virtual particles such that the charge transmitted by them, αN^* , with $\alpha = \sqrt{C_3/C_1}$, gets as close as possible to the net charge of real electrons N . Here the square brackets [...] denote the rounding function. We have also assumed that $C_1, C_3 > 0$, and $C_2^2 > C_1 C_3$. The approximation (4) is valid if the conditions

$$\frac{C_1 |C_1 C_4 - C_2 C_3|}{12 C_2^3} \left(\frac{N}{C_1 t} - 1 \right)^2 \lesssim 1, \quad t \gg \tau_r, \quad |N| \gg 1 \quad (5)$$

are fulfilled [50]. The first condition implies that the approximation (4) works in the vicinity of the maximum of the distribution $\mathcal{P}_N(t)$, occurring close to $t = N/C_1$, but may fail in the tails of the distribution. At short times the expression (4) behaves as $t^{|N^*|-1}$. Provided that $|C_3 - C_1| \lesssim C_1$, it reproduces the scaling of the exact distribution $\mathcal{P}_N(t) \sim t^{|N|-1}$ for small values of N . In this case the last of the conditions (5) may be relaxed. In the long time limit Eq. (4) correctly reproduces the exponential decay of $\mathcal{P}_N(t)$ predicted by the exact theory [22], but may provide an inaccurate decay rate if the first of the conditions (5) is violated. Next, in the Gaussian limit $C_3 \rightarrow 0$ the distribution (4) reduces to the form

$$\mathcal{P}_N(t) = \frac{|N| e^{-\frac{(N-C_1)t^2}{2C_2t}}}{\sqrt{2\pi C_2 t^{3/2}}}, \quad (6)$$

well known from the theory of Brownian motion [1,2], and for $C_3 = C_1$ Eq. (4) gives the random walk result [3,51]

$$\mathcal{P}_N^{\text{arw}}(t) = \frac{|N|}{t} e^{-(\Gamma_+ + \Gamma_-)t} \left(\frac{\Gamma_+}{\Gamma_-}\right)^{\frac{N}{2}} I_N(2\sqrt{\Gamma_+ \Gamma_-}t), \quad (7)$$

with $\Gamma_{\pm} = (C_2 \pm C_1)/2$. We also note that the total probability of reaching a given threshold $A_N = \int_0^{\infty} dt \mathcal{P}_N(t)$ is equal to 1 for $N > 0$ and is less than 1 for $N < 0$.

The approximate distribution (4) satisfies the fluctuation relation

$$\frac{\mathcal{P}_N(t)}{\mathcal{P}_{-N}(t)} = \frac{A_N}{A_{-N}} = \left(\frac{C_2 + \sqrt{C_1 C_3}}{C_2 - \sqrt{C_1 C_3}}\right)^{|N| \sqrt{C_1/C_3}}, \quad (8)$$

which does not require the system to be in equilibrium or to exhibit detailed balance, and relies only on the conditions (5). In the limit $t \gg \tau_r$, and provided the system has a well-defined temperature T , one can also prove an exact fluctuation relation [10,11,17,23,36,56],

$$\mathcal{P}_N(t)/\mathcal{P}_{-N}(t) = \exp[N e V_b / k_B T], \quad (9)$$

which is a consequence [50] of the fluctuation theorem for the electron transport [38–41] and remains valid for quantum conductors described by the Schrödinger equation. Equations (8) and (9) are close in the common range of validity. They become equivalent, e.g., for a Gaussian equilibrium stochastic process describing charge transport through an Ohmic resistor, in which case $C_2 = 2k_B T C_1 / e V_b$ and $C_3 \rightarrow 0$, and for a biased tunnel junction, for which $C_3 = C_1$ and $C_2 = C_1 \coth[e V_b / 2k_B T]$.

Discussion.—We have determined the transition rates between the charge states of the double dot, given in the caption of Fig. 2, in the usual way by counting the number of corresponding transitions. The numerical calculations based on the exact theory [22,23] with these rates agree with the experiment very well, see Fig. 3.

Next, we test the approximate expression (4). Having determined the rates, we have used the full counting statistics formalism [54,57] and found the first four cumulants of the charge distribution, $C_1 = 4.60$, $C_2 = 9.27$, $C_3 = 2.18$, $C_4 = 3.96$ Hz. As a consistency check, we have also determined the cumulants directly from the measured distributions of the number of transmitted electrons $P_t(N)$, and obtained the same values within ± 0.2 Hz, which is compatible within the statistical uncertainty. The system relaxation time is given by the inverse of the eigenvalue of the transition rates matrix, which has the real part closest to zero among its nonzero

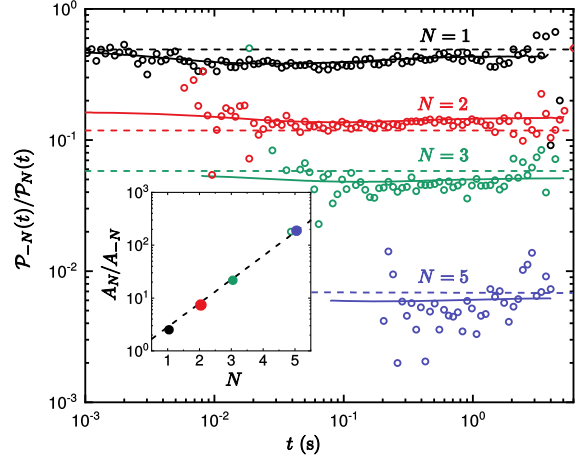


FIG. 4. First-passage-time fluctuation relation. The ratio $\mathcal{P}_N(t)/\mathcal{P}_{-N}(t)$ for several values of N . Symbols are the experimental data, solid lines the exact theory [22], dashed lines the approximation (8). Inset: the ratio of the total probabilities integrated over time, A_N/A_{-N} ; symbols are the experimental data, dashed line is approximation (8).

eigenvalues, and equals $\tau_r = 8.7$ ms [58]. With these values of the cumulants the first of the conditions (5) is fulfilled at $t \rightarrow \infty$ and the expression (4) fits the experimental data very well in the long time limit, see Fig. 3. The first two of the conditions (5) are violated in the shaded areas of Figs. 3(a), 3(b). We find that Eq. (4) fits the experimental data rather well outside these areas even for small values of the threshold $|N| = 1, 2$, which is explained by the relatively small difference between the cumulants C_1 and C_3 . We have found that at another value of the bias voltage, at which the difference between C_1 and C_3 is bigger, Eq. (4) has worked only for sufficiently large $|N|$ [50].

We have also tested the fluctuation relation (8) by comparing it to the experimental data and to the numerics based on the exact theory [22,23]. The result of this comparison is shown in Fig. 4. We have again found that the numerics provides a very accurate match with the data. The approximation (8), although less accurate, also describes the experiment rather well. The exact numerical analysis reveals the approximate nature of the fluctuation relations (8), (9) for nonequilibrium systems with broken detailed balance, like our double dot. Indeed, the solid lines in Fig. 4, showing the exact results, slightly deviate from constant values. We also note that our double dot is suitable for testing the fluctuation relations for Markovian systems with hidden states [59,60].

Conclusion.—We have measured the distribution of the first-passage times for electrons tunneling between the two islands of a double dot. Our experimental results perfectly agree with the predictions of an exact theory [22,23]. We have also proposed a simple approximation for the distribution of the first passage times (4), which accounts for

the non-Gaussian statistics of electron tunneling via the third cumulant of the distribution of the number of transmitted electrons. This universal result applies to any stochastic process and captures the leading non-Gaussian correction to the central limit theorem. The approximation (4) fits the experimental data quantitatively without free parameters. Finally, we have experimentally verified a fundamentally important fluctuation relation for the first passage times (8).

We acknowledge the provision of facilities by Aalto University at OtaNano Micronova Nanofabrication Centre and computational resources provided by Aalto Science-IT project. We thank Matthias Gramich and Libin Wang for technical assistance, and Abhishek Dhar and Izaak Neri for fruitful discussions. This work is partially supported by Academy of Finland, Projects No. 284594, No. 272218, and No. 275167 (S. S., D. S. G., J. T. P., and J. P. P.), by the European Research Council (ERC) under the European Union's Horizon 2020 research and innovation programme under Grant Agreement No. 742559 (SQH), by JSPS Grants-in-Aid for Scientific Research (JP16H02211 and JP17K05587) (K. S.) and by German Research Foundation (DFG) Grant No. KH 425/1-1, the Russian Foundation for Basic Research under Grant No. 17-52-12044 (I. M. K.). In the part concerning the fluctuation relations, the work was supported by Russian Science Foundation under Grant No. 17-12-01383 (I. M. K.).

*To whom all correspondence should be addressed.
sshilpi916@gmail.com

- [1] M. V. Smoluchowski, *Phys. Z.* **16**, 318 (1915).
- [2] E. Schrodinger, *Phys. Z.* **16**, 289 (1915).
- [3] S. Redner, *A Guide to First-Passage Processes* (Cambridge University Press, Cambridge, England, 2001).
- [4] R. Metzler, S. Redner, and G. Oshanin, *First-Passage Phenomena and Their Applications* (World Scientific, Singapore, 2014).
- [5] O. Artime, N. Khalil, R. Toral, and M. San Miguel, *Phys. Rev. E* **98**, 042143 (2018).
- [6] X. Yang, C. Liu, Y. Li, F. Marchesoni, P. Hänggi, and H. P. Zhang, *Proc. Natl. Acad. Sci. U.S.A.* **114**, 9564 (2017).
- [7] A. Szabo, K. Schulten, and Z. Schulten, *J. Chem. Phys.* **72**, 4350 (1980).
- [8] R. Zwanzig, A. Szabo, and B. Bagchi, *Proc. Natl. Acad. Sci. U.S.A.* **89**, 20 (1992).
- [9] E. A. Galburt, S. W. Grill, A. Wiedmann, L. Lubkowska, J. Choy, E. Nogales, M. Kashlev, and C. Bustamante, *Nature (London)* **446**, 820 (2007).
- [10] H. Qian and X. S. Xie, *Phys. Rev. E* **74**, 010902(R) (2006).
- [11] M. Bauer and F. Cornu, *J. Stat. Phys.* **155**, 703 (2014).
- [12] O. Benichou, C. Chevalier, J. Klafter, B. Meyer, and R. Voituriez, *Nat. Chem.* **2**, 472 (2010).
- [13] S. Chandrasekhar, *Astrophys. J.* **97**, 263 (1943).
- [14] S. N. Majumdar, *Curr. Sci.* **89**, 93 (2006).
- [15] A. Wald, *Sequential Analysis* (Dovel Publications, Mineola, 1973).
- [16] E. D. Siggia and M. Vergassola, *Proc. Natl. Acad. Sci. U.S.A.* **110**, E3704 (2013).
- [17] É. Roldán, I. Neri, M. Dörpinghaus, H. Meyr, and F. Jülicher, *Phys. Rev. Lett.* **115**, 250602 (2015).
- [18] V. Tejedor, R. Voituriez, and O. Bénichou, *Phys. Rev. Lett.* **108**, 088103 (2012).
- [19] C. Mejía-Monasterio, G. Oshanin, and G. Schehr, *J. Stat. Mech.* (2011) P06022 (2011).
- [20] J.-P. B. R. Chicheportiche, *First-Passage Phenomena and Their Applications*, edited by R. Metzler, G. Oshanin, and S. Redner (World Scientific, Singapore, 2014).
- [21] J. Perelló, M. Gutiérrez-Roig, and J. Masoliver, *Phys. Rev. E* **84**, 066110 (2011).
- [22] K. Saito and A. Dhar, *Europhys. Lett.* **114**, 50004 (2016).
- [23] K. Ptasiński, *Phys. Rev. E* **97**, 012127 (2018).
- [24] I. Neri, É. Roldán, and F. Jülicher, *Phys. Rev. X* **7**, 011019 (2017).
- [25] T. R. Gingrich and J. M. Horowitz, *Phys. Rev. Lett.* **119**, 170601 (2017).
- [26] J. P. Garrahan, *Phys. Rev. E* **95**, 032134 (2017).
- [27] P. Hänggi, P. Talkner, and M. Borkovec, *Rev. Mod. Phys.* **62**, 251 (1990).
- [28] M. Albert, C. Flindt, and M. Büttiker, *Phys. Rev. Lett.* **107**, 086805 (2011).
- [29] D. Dasenbrook, C. Flindt, and M. Büttiker, *Phys. Rev. Lett.* **112**, 146801 (2014).
- [30] W. Lu, Z. Ji, L. Pfeiffer, K. W. West, and A. J. Rimberg, *Nature (London)* **423**, 422 (2003).
- [31] T. Fujisawa, T. Hayashi, R. Tomita, and Y. Hirayama, *Science* **312**, 1634 (2006).
- [32] S. Gustavsson, R. Leturcq, B. Simović, R. Schleser, T. Ihn, P. Studerus, K. Ensslin, D. C. Driscoll, and A. C. Gossard, *Phys. Rev. Lett.* **96**, 076605 (2006).
- [33] C. Flindt, C. Fricke, F. Hohls, T. Novotný, K. Netočný, T. Brandes, and R. J. Haug, *Proc. Natl. Acad. Sci. U.S.A.* **106**, 10116 (2009).
- [34] S. N. Majumdar, *Physica (Amsterdam)* **389A**, 4299 (2010).
- [35] M. Dörpinghaus, É. Roldán, I. Neri, H. Meyr, and F. Jülicher, in *IEEE International Symposium on Information Theory (ISIT)* (IEEE, New York, 2017).
- [36] M. Dörpinghaus, I. Neri, É. Roldán, H. Meyr, and F. Jülicher, [arXiv:1801.01574](https://arxiv.org/abs/1801.01574).
- [37] S. Singh, É. Roldán, I. Neri, I. M. Khaymovich, D. S. Golubev, V. F. Maisi, J. T. Peltonen, F. Jülicher, and J. P. Pekola, *Phys. Rev. B* **99**, 115422 (2019).
- [38] J. Tobiska and Y. V. Nazarov, *Phys. Rev. B* **72**, 235328 (2005).
- [39] H. Förster and M. Büttiker, *Phys. Rev. Lett.* **101**, 136805 (2008).
- [40] Y. Utsumi and K. Saito, *Phys. Rev. B* **79**, 235311 (2009).
- [41] D. Andrieux, P. Gaspard, T. Monnai, and S. Tasaki, *New J. Phys.* **11**, 043014 (2009).
- [42] Y. Utsumi, D. S. Golubev, M. Marthaler, K. Saito, T. Fujisawa, and G. Schön, *Phys. Rev. B* **81**, 125331 (2010).
- [43] B. Küng, C. Rössler, M. Beck, M. Marthaler, D. S. Golubev, Y. Utsumi, T. Ihn, and K. Ensslin, *Phys. Rev. X* **2**, 011001 (2012).
- [44] In our analysis, we do not consider cotunneling or Andreev tunneling due to high resistance of all junctions.

- [45] B. Derrida, E. Domany, and D. Mukamel, *J. Stat. Phys.* **69**, 667 (1992).
- [46] G. Schütz and E. Domany, *J. Stat. Phys.* **72**, 277 (1993).
- [47] O. Golinelli and K. Mallick, *J. Phys. A* **39**, 12679 (2006).
- [48] B. Derrida, *J. Stat. Mech.* (2007) P07023.
- [49] M. E. Cates and M. R. Evans, *Soft and Fragile Matter: Nonequilibrium Dynamics, Metastability and Flow* (CRC Press Taylor & Francis Group, Boca Raton, 2000).
- [50] See Supplemental Material at <http://link.aps.org/supplemental/10.1103/PhysRevLett.122.230602> for further details, which includes Refs. [1–3,22,23,51–54].
- [51] W. Feller, *An Introduction to Probability Theory and Its Applications* (John Wiley, New York, 1957).
- [52] L. S. Levitov, H. Lee, and G. B. Lesovik, *J. Math. Phys. (N.Y.)* **37**, 4845 (1996).
- [53] A. J. F. Siegert, *Phys. Rev.* **81**, 617 (1951).
- [54] D. A. Bagrets and Y. V. Nazarov, *Phys. Rev. B* **67**, 085316 (2003).
- [55] The first three cumulants are defined in the standard way as $C_1 = \lim_{t \rightarrow \infty} \langle N \rangle / t$, $C_2 = \lim_{t \rightarrow \infty} \langle (N - C_1 t)^2 \rangle / t$ and $C_3 = \lim_{t \rightarrow \infty} \langle (N - C_1 t)^3 \rangle / t$. The angular brackets imply the averaging with the distribution $P_t(N)$.
- [56] P. L. Krapivsky and S. Redner, *J. Stat. Mech.* (2018) 093208.
- [57] A. Wachtel, J. Vollmer, and B. Altaner, *Phys. Rev. E* **92**, 042132 (2015).
- [58] This timescale is larger than the electron-phonon relaxation time $\sim 10^{-6}$ s, and electron-electron relaxation time $\sim 10^{-9}$ s.
- [59] B. Altaner, M. Polettini, and M. Esposito, *Phys. Rev. Lett.* **117**, 180601 (2016).
- [60] M. Polettini and M. Esposito, *Phys. Rev. Lett.* **119**, 240601 (2017).